High temporal and high spatial resolution MR angiography (4D-MRA)

Zeitlich und räumlich hochaufgelöste MR Angiografie („4D-MRA“)

Authors D. R. Hadizadeh, C. Marx, J. Gieseke, H. H. Schild, W. A. Willinek

Affiliation Radiology, University of Bonn

Key words
- vascular
- MR-angiography
- imaging sequences
- AVM
- arteries

Abstract

In the first decade of the twenty-first century, whole-body magnetic resonance scanners with high field strengths (and thus potentially better signal-to-noise ratios) were developed. At the same time, parallel imaging and “echo-sharing” techniques were refined to allow for increasingly high spatial and temporal resolution in dynamic magnetic resonance angiography (“time-resolved” = TR-MRA). This technological progress facilitated tracking the passage of intra-venously administered contrast agent boluses as well as the acquisition of volume data sets at high image refresh rates (“4D-MRA”). This opened doors for many new applications in non-invasive vascular imaging, including simultaneous anatomic and functional analysis of many vascular pathologies including arterio-venous malformations. Different methods were established to acquire 4D-MRA using various strategies to acquire k-space trajectories over time in order to optimize imaging according to clinical needs. These include “keyhole”-based techniques (e. g. 4D-TRAK), TRICKS – both with and without projection – and HYPR-reconstruction, TREAT, and TWIST. Some of these techniques were first introduced in the 1980 s and 1990 s, were later enhanced and modified, and finally implemented in the products of major vendors. In the last decade, a large number of studies on the clinical applications of TR-MRA was published. This manuscript provides an overview of the development of TR-MRA methods and the 4D-MRA techniques as they are currently used in the diagnosis, treatment and follow-up of vascular diseases in various parts of the body.

Key statements

- 4D-MRA, which differs according to manufacturer, generates high temporal and spatial resolution MRA volume data sets.
- Key differences in 4D-MRA techniques concern the sequence of the acquisition of k-space portions.
- Central k-space portions define image contrast and are thus repetitively scanned with 4D-MRA.
- Numerous clinical applications of 4D-MRA are already documented in the literature.

Citation Format:
- Hadizadeh DR., Marx C, Gieseke J et al. High temporal and high spatial resolution MR angiography (4D-MRA). Fortschr Röntgenstr 2014; 186: 847–859

Zusammenfassung

Im ersten Jahrzehnt des 21. Jahrhunderts wurden Ganzkörper-Magnetresonanztomografen mit höheren Feldstärken (und damit potenziell besserem Signal-zu-Rausch-Verhältnis) entwickelt. Dies und die nahezu zeitgleiche Entwicklung bzw. Verfeinerung von Techniken wie der parallelen Bildgebung und „Echo-sharing“ erlaubten ein zunehmend höheres räumliches und zeitliches Auflösungsvermögen in der dynamischen Magnetresonanzangiografie („Time-resolved“ = TR-MRA). Somit konnten erstmals sowohl die Passage eines Kontrastmittelbolus mit einer angemessenen räumlichen Auflösung verfolgt als auch Volumendatensätze mit hohen Bildauffrischungsraten erzeugt werden („4D-MRA“). Damit eröffneten sich neue Optionen der nicht invasiven Gefäßdiagnostik, wie beispielsweise die gleichzeitige anatomische und funktionelle Analyse von Gefäßmalformationen. Es wurden zahlreiche unterschiedliche Methoden eingeführt, bei denen die Akquisitionen der k-Raum-Trajektorien strategisch unterschiedlich

received 6.1.2014
accepted 8.5.2014

Bibliography
DOI http://dx.doi.org/10.1055/s-0034-1366661
Published online: 23.6.2014
Fortschr Röntgenstr 2014; 186: 847–859 © Georg Thieme Verlag KG Stuttgart · New York · ISSN 1438-9029

Correspondence
Dr. Dariusch Reza Hadizadeh
Radiology, University of Bonn
Sigmund-Freud-Str. 25
53113 Bonn
Germany
Tel.: ++ 49/2 28/28 71 58 75
Fax: ++ 49/2 28/28 71 60 93
dr.hadizadeh@uni-bonn.de

über den Akquisitionszeitraum verteilt wurden, um optimale klinische Ergebnisse zu erlangen. Dazu zählten beispielsweise Verfahren wie „Keyhole"-basierte Techniken (z. B. 4D-TRAK), TRICKS mit und ohne Projektions- und HYPR-Rekonstruktion, TREAT und TWIST. Einige dieser Techniken wurden bereits in den 80er- und 90er-Jahren vorgestellt, in der Folge weiterentwickelt und modifiziert und schließlich in handelsübliche MR-Tomografen der verschiedenen Hersteller implementiert. In der letzten Dekade wurden schließlich zahlreiche Studien zu klinischen Anwendungen der TR-MRA vorgestellt. Dieses Manuskript bietet eine Übersicht über die Entwicklung der TR-MRA-Verfahren und die gegenwärtig eingesetzten 4D-MRA-Techniken wie sie derzeit Ihren klinischen Einsatz bei der Diagnose, Behandlung und bei Verlaufsuntersuchungen von Gefäßerkrankungen in unterschiedlichen Körperregionen finden.

Introduction

MR angiography strategies have undergone constant refinement since the introduction of contrast-enhanced MR angiography by Prince et al. in 1993 and dynamic imaging using the "keyhole" method by van Vaals et al. and Jones et al. that same year. In particular, parallel imaging had a large impact on increasing the temporal efficiency of data collection sufficiently dynamically showing the contrast medium bolus passage in the blood vessel with high spatial resolution [1 – 5]. For the simultaneous imaging of flow dynamics and vascular anatomy, the invasive method of catheter angiography in the form of digital subtraction angiography (DSA) is the reference standard against which all new methods have to compete.

Dynamic information about blood flow in vessels is essential for functional analysis of arterial inflow and venous outflow of vascular malformations, for example. However, TR-MRA can also be helpful when it is necessary to image multiple vascular territories simultaneously while administering low doses of contrast medium, e. g. in children and patients who can tolerate only short examination times [6, 7]. 4D-MRA is generally useful for every clinical problem involving a short arteriovenous transit time, for example in the pulmonary artery flow path, where it has ben used to investigate arteriovenous fistulae and shunts [8 – 13]. This review provides an overview of the temporal resolution MR angiography techniques currently used routinely and their development, while presenting various clinical applications in which these techniques have already been employed successfully. Diagnosing cerebral arteriovenous malformations (cAVM) is an example of a key clinical application for comparing individual methods, since these malformations can be examined using all of the techniques described in the article, and data from prospective studies have already been published and in turn cited in this article.

The development of temporal resolution MR angiography techniques

The first temporal resolution MR sequences were developed to roughly image the bolus passage of contrast agents and thereby ascertain bolus arrival time. For this purpose, T1-weighted gradient echo techniques single-thick slice- (known as 2D-MRA) were created. At that time, however, significant compromises had to be made in terms of spatial resolution to facilitate achieving the requisite very short time intervals of 1 – 2 seconds [14 – 16].

This idea of dynamically tracking a contrast medium bolus (integrated with a mask subtraction of non-contrast images) is indispensable for planning and facilitating precise temporal initiation of static sequences such as high spatial resolution volume data sets (3D-CEMRA), which absolutely require precise "timing", i. e. a precise starting time (fluoroscopic triggering).

T1-weighted 2D-multi-slice and 3D-gradient echo sequences are generally suited for showing the arrival of a contrast medium bolus with a high signal-to-noise ratio. However, to achieve a high image refresh rate in this process, it is necessary to limit the k-space portions that are actually scanned. First, image acquisition was accelerated using above all the symmetry characteristics of the k-space. Major advancements in the acceleration of dynamic sequences were then achieved through the introduction of parallel imaging [17 – 19], the use of higher field strengths with a more favorable signal-to-noise ratio and the use of complex, strategic k-space acquisition schemes. One such scheme is "echo sharing", which is the practice of strategically distributing k-space acquisition over the sequence duration and using a certain temporal interpolation to reconstruct k-space. What is critical here is that the portion of k-space (central portion) that essentially determines image contrast is scanned at a higher frequency than k-space portions (peripheral portions) that are less significant to image contrast. This allows contrast change to be mapped over time even if only a small portion of k-space is actually acquired per dynamic phase [20, 21]. Through the use of higher field strengths and improved coils [11, 22 – 24] sequences were established in the last decade that simultaneously facilitate both high temporal and spatial resolution in dynamic vascular imaging. The result was a steady increase in publications on the field of 4D-MRA which continues to this day (**Fig. 1a**). Because the development of these complex techniques required close cooperation between clinical institutions and commercial partners, the various "echo-sharing" techniques were used mostly in a manufacturer-specific manner (**Table 1**). These techniques are listed in this review according to method.

As mentioned above, that was used to accelarate dynamic imaging cAVM are especially well suited for testing the effectiveness of 4D-MRA. This clinical picture was therefore examined in clinical studies using each of the methods introduced, resulting in data that facilitates good comparison. The currently employed "echo-sharing" techniques are introduced below and compared using the example of cAVM imaging in view of the good body of data:

"Keyhole"-based techniques

In 1993, the same year contrast-enhanced 3D-CEMRA was introduced by Prince et al., Van Vaals et al. and Jones et al. described separate techniques which involved repetitively scanning the central k-space, while acquiring the peripheral k-space only once. Afterwards, missing information from the one-time scanning of the peripheral k-space is added to each

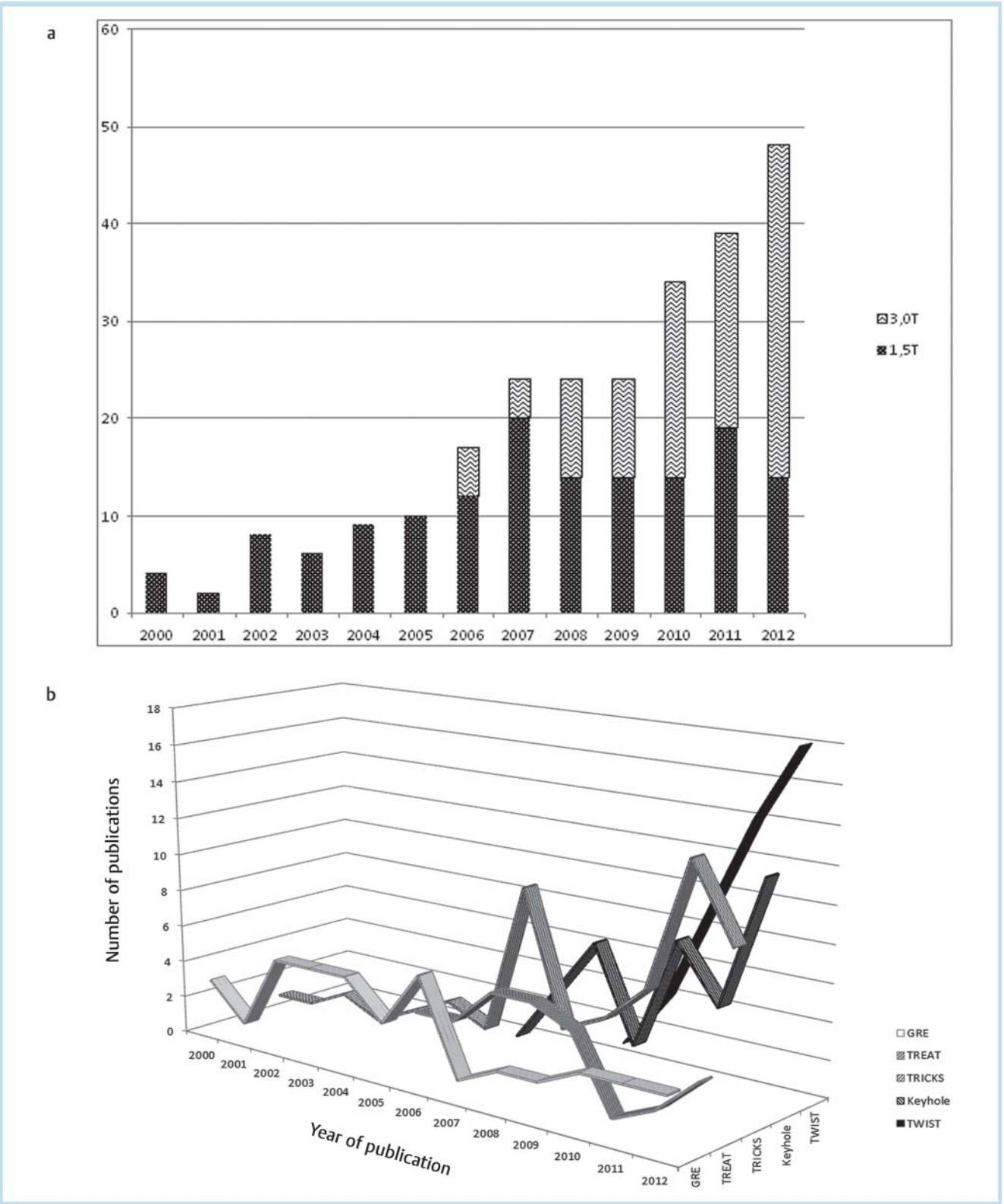

Fig. 1 Original publications on time-resolved MRA between 2000 and 2012; **a** Number of publications related to field strength; **b** Publications broken down by TR-MRA technique.

of the incomplete, central, dynamic data sets to finally generate complete k-space data sets for each point in time [2, 3]. The complete data set from which the missing k-space portions are “borrowed” is identified as the reference data set and is usually acquired after the dynamic phases upon completion of the sequence. In only 1993 Van Vaals declared that the “keyhole" technique should be combined with

TR-MRA technique	year	field strength	manufacturer
keyhole	1993	1.5 T	Philips Healthcare, Best, Netherlands
4D-TRAK	2008	1.5 T	Philips Healthcare, Best, Netherlands
	2008	3.0 T	Philips Healthcare, Best, Netherlands
4D-TRAK+	2011	3.0 T	Philips Healthcare, Best, Netherlands
TRICKS	1996	1.5 T	General Electric Healthcare, Milwaukee, WI, USA
PR-TRICKS	2002	1.5 T	General Electric Healthcare, Milwaukee, WI, USA
HYPR PR-TRICKS	2006	1.5 T	General Electric Healthcare, Milwaukee, WI, USA
	2007	3.0 T	General Electric Healthcare, Milwaukee, WI, USA
TREAT	2005	1.5 T	Siemens Healthcare, Erlangen, Deutschland
	2006	3.0 T	Siemens Healthcare, Erlangen, Deutschland
TWIST	2008	1.5 T	Siemens Healthcare, Erlangen, Deutschland
	2010	3.0 T	Siemens Healthcare, Erlangen, Deutschland

[1] Year = year first described in technical literature; Manufacturer = manufacturer of the MR systems on which the indicated technique was implemented at the time

Table 1 Time-resolved contrast-enhanced TR-MRA techniques.[1]

other acceleration methods "*based on different principles*" to achieve even higher acceleration.

This predicted development was realized in the subsequent two decades as a result of different techniques facilitating accelerated data acquisition actually being developed. "Temporal resolution MR angiography with CENTRA-Keyhole" (4D-TRAK, Philips Healthcare, Best, Netherlands) represents the combination of multiple acceleration techniques with keyhole imaging and already enjoys routine clinical use. This technique combines the keyhole principle with a randomized acquisition of central k-space data (CENTRA-Keyhole), parallel imaging (SENSE) with high acceleration factors and half-Fourier acquisition [25 – 27]. Further refinement of the technique involves subdividing the central k-space partition (the "keyhole window") into three smaller fractions, which are likewise acquired alternatingly (temporal resolution MR angiography with keyhole and view sharing [4D-TRAK+]; **Fig. 2a**) [28].

Keyhole techniques were used for examining the abdomen, thorax and extremities as well as the head and neck at 1.5 T [29 – 36] and the pelvis, thorax and extremities as well as the head and neck at 3.0 T [26, 28, 37 – 47].

For example, these techniques allowed the imaging of surgically created shunt connections between the superior vena cava and the pulmonary artery during Fontan procedures. This technique was likewise used to image dialysis shunts or to acquire purely arterial images of the lower leg region in cases of asymmetrical contrast perfusion.

In principle limitations in the complete suppression of the venous signal can appear with keyhole-based techniques if too small a fraction of the central k-space is selected. Caution is advised when using very high compression factors with 4D-TRAK+, since a flickering artefact can appear in cinematic view [28]. This is based on the fact that 100 % symmetrical boundary conditions are never present in k-space due to noise and that when high compression factors are present only positive or negative central k-space portions can be used for image reconstruction on an alternating basis. This results in deviations, albeit minor, in image contrast ("flickering"). Taking these limitations into account, a temporal resolution of 572 ms at a simultaneous spatial resolution of (1.1 × 1.1 × 1.1) mm³ was achieved when 4D-TRAK+ was used for examining cAVM, for example, while imaging all cranial blood vessels [41].

TRICKS

In 1996 Korosec et al. described a technique named 3D-TRICKS (time-resolved imaging of contrast kinetics) [42] in which different k-space portions are acquired over a period of time, and missing portions are borrowed from prior or subsequent data sets (**Fig. 2b**) in the sense of a temporal interpolation [43].

The peripheral (higher frequency) portions of k-space (B, C and D) are scanned three times less frequently than the central (lower frequency) portions (A). Using these k-space fractions, data collection is repeated according to the following sequence, for example: D, A, C, A, B, A. In addition, the entire k-space is scanned at the beginning and end of the TR-MRA sequence with all of its four portions.

Various enhancements to this acquisition scheme were subsequently developed. For example, (PR)-TRICKS uses radial projection reconstructions on the $k_x k_y$ plane combined with a variable k-space scanning rate for accelerated dynamic data acquisition [44]. Cartesian coding is then employed in the slice encoding direction. The next step was "HYPR TRICKS", which added "highly-constrained back-projection reconstruction" (HYPR) to improve the dynamic low-frequency data of the TRICKS-algorithm as well as (by means of high-frequency data) the signal-to-noise ratio and thus both temporal as well as spatial resolution with the aid of an additional high-resolution data set following venous filling [45, 46]. Combining all of these methods (HYPR PR-TRICKS), however, results in high sensitivity to patient movements, which can in turn compromise image quality [47]. It is therefore necessary to precisely weigh the advantages and disadvantages of these highly complex acquisition schemes to find the ideal compromise for the particular clinical application. Applications for the abdomen, thorax, extremities and head and neck at 1.5 T [48 – 64] and for the head and neck as well as the extremities at 3.0 T [65 – 72] have been published.

Literature contains examples of clinical applications of TRICKS-4D-MRA for pulmonary angiographies, for diagnosing carotid-cavernous sinus fistulae as well as for improved diagnosing of diseases in the arteries of the lower legs, particularly in patients with diabetes mellitus. As with all 4D-MRA techniques, limitations of the TRICKS technique can appear through temporal interpolation.

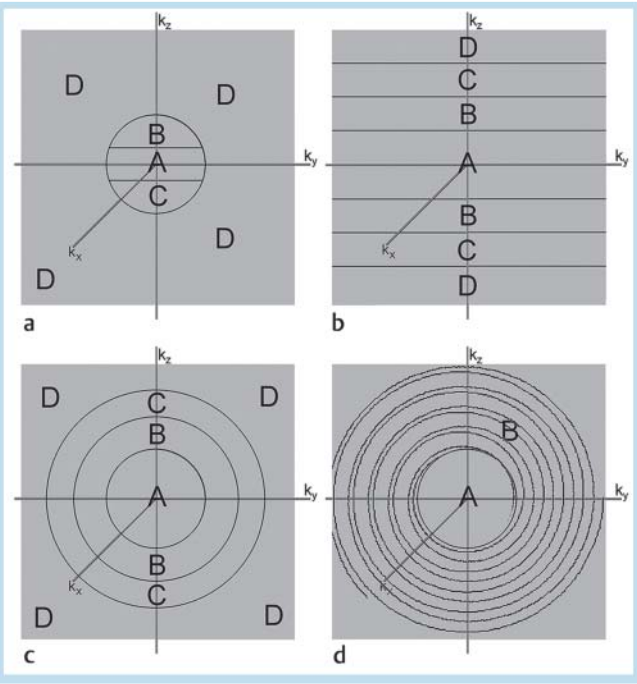

Fig. 2 K-space acquisition using various 4D-MRA techniques; K-space acquisition schemes in phase encoded (k_y), slice encoded (k_z) and frequency encoded direction (k_x). A "zero filling" non-acquired k-space regions is not illustrated in graphics a through d. **a** Keyhole acquisition with view-sharing (4D-TRAK+): During dynamic imaging phase, either segment A or one of the segments B and C is scanned on an alternating basis. Area D is scanned following the dynamic acquisition phase and added to all dynamic acquisitions. **b** 3D-TRICKS: Initial concept with four equally sized Ky-segments (containing the same number of (k_y, k_z) points) with A, B, C and D. Either segment A or one of the segments B, C and D is scanned on an alternating basis. Complete k-spaces are yielded by putting together all temporally neighboring segments A, B, C and D. **c** TREAT: Concept with n possible regions. The regions A, B, C and D contain the same number of (k_y, k_z) points and are divided according to their distance from the center of the k-space into the innermost segment A and the additional peripherally located segments B, C and D. Either segment A or one of the segments B, C and D are scanned on an alternating basis, and complete K-spaces are yielded in turn by putting together the temporally neighboring segments A, B, C and D. **d** TWIST: In each dynamic phase the central portion of k-space is scanned, while only a fraction of the peripheral region B is scanned. This region is comprised of elliptical trajectories interwoven ("twisted") with one another. Missing data needed for assembling a complete k-space are taken from the respective temporally neighboring dynamic phases.

In the case of HYPR-TRICKS techniques, low data density ("sparsity") can result in signal fluctuations. It was shown that very high image refresh rates can be achieved with HYPR-TRICKS while employing to some extent very complex reconstruction algorithms and extremely low portions of actually acquired data. Based on the clinical application example of examining cAVM, an image refresh rate of 0.8 s at a voxel size of $0.5 \times 0.75 \times 4 mm^3$ was achieved using a TRICKS algorithm [69].

TREAT

TREAT (time-resolved echo-shared angiography technique) was first described in 2005 by Fink et al. and divides the k-space into n regions (for example, regions A, B, C and D when n = 4) [73]. Each region covers an equal portion of k-space and thus the same number of (k_y, k_z) points (**Fig. 2c**).

Following complete k-space acquisition, the scanning of the central segment A and one of the peripheral segments B, C or D alternates similar to the scheme employed in the TRICKS technique. To reconstruct the images, complete k-space data is generated by summarizing the k-space data of the next consecutive acquisitions.

For a segmentation pattern with n segments, a complete data set can then be reconstructed in intervals of 2 • TA/n (TA being the time needed for obtaining a complete data set). However, as the number of segments increases, the signal intensity is distributed further over the image plane, resulting in increasingly less defined smaller blood vessels.

Numerous studies use this technique on various regions of the body at 1.5 T [12, 73 – 83] and in the head and neck at 3.0 T [85 – 88]. Among the published indications for these examinations are the imaging of pathological flow conditions with the occurrence of endoleaks in cases of aortic prostheses, [76] as well as diagnosing pulmonary embolisms [83] or subclavian steal syndromes [84]. Possible limitations arise from the fact that each data set is reconstructed from similarly sized portions of k-space partitions from various points in time and is thus interpolated over time. This particularly effects the imaging of small blood vessels to the extent that neighboring small arteries and veins can no longer be distinguished from one another. Using the TREAT algorithm, a temporal resolution of 1.5 s per 3 D data set with a simultaneous spatial resolution $1.2 \times 1.0 \times 4 mm^3$ was achieved when imaging cAVM [88].

TWIST

The details of the TWIST technique (time-resolved imaging with stochastic trajectories) were reported by Vogt, Lim and Song over the period of 2007 to 2009 [89 – 91]. In this technique, all points in the k-space are sorted according to their radial distance from the center of the k-space. A critical radial distance can be defined around the k-space and subdivided into two subareas, a central region A (low-frequency portions) and a peripheral region B (high-frequency portions) (**Fig. 2d**).

During data acquisition, the data of the entire k-space is gathered only once, either at the beginning or end of the sequence. For the dynamic phase of image acquisition, the entire region A within each time window is acquired, while one of n portions is scanned from region B, and missing data points are taken from temporally adjacent acquisitions of region B for complete k-space reconstruction.

In this process, the k-space trajectories of region B follow a spiral pattern on the k_y-k_z plane, with the trajectories from region B being intertwined with one another, giving the sequence its name. With TWIST, acceleration is based on both the size of region A and the density of trajectories in region B. This technique has been used on the abdomen, thorax, extremities as well as on the head and neck at both 1.5 T [92 – 96] and 3.0 T [92, 97 – 104]. TWIST has likewise been used to image ovarian vein reflux [92] as well as thoracic venous outflow obstructions [94], examine pathologies of the abdominal aorta [100] and successfully diagnose changes in

flow conditions in cases of peripheral occlusive arterial disease [97]. However, the complex acquisition pattern of TWIST data recording with its data collection interwoven over the acquisition time poses special challenges for assigning artefacts to certain k-space portions, which is made even more difficult by the fact that artefacts are always present in multiple consecutive data sets because of the temporal interpolation reconstructed of the data. Regardless of these limitations, patients with cAVM, for example, have been successfully examined at a temporal resolution of 0.58 s and a voxel size of $(1.6 \times 1.6 \times 1.6)mm^3$ [103]

Summary and supplemental technical observations

While implementing TR-MRA demands high standards for software and hardware, current tomography machines from major manufacturers implement high-quality manufacturer-specific TR-MRA sequences. Each of these techniques has its pros and cons that would make particular methods appear to be optimal for particular cases.

It must be emphasized that images reconstructed from complex temporally intertwined data generally do not correspond to any exact visualization of a single time point (temporal interpolation). However, the central k-space portions used exclusively at a particular point in time are essential for the image contrast of the corresponding image so that the contrast curve can be realistically mapped.

Because of the potential cons of this temporal interpolation, Riederer et al. have introduced the concept of "temporal footprint" of high temporal resolution sequences. This concept describes the period of time that is needed to acquire a complete k-space data set, i. e. the entire k-space portions. Dividing the k-space into multiple portions in the process of time-resolved imaging would produce the following "temporal footprint" in which the exemplary constellation has 4 equal-sized portions A-D (acquisition duration 1 s each, A = central k-space portion):

Example 1 (**Fig. 3a**): Acquisition in the sequence A, B, C, D...; central k-space portions are acquired every 4s; the temporal footprint is the product of the summation of individual k-space portions A-D, with the acquisition time between each being omitted, resulting in a temporal footprint = 4 s.

Example 2 (**Fig. 3b**): Acquisition in the sequence A, B, A, C, A, D...; central k-space portions are acquired alternatingly with peripheral k-space portions B, C or D every 2 s. The temporal footprint is, in contrast, the product of the summation of individual k-space portions A-D plus the intermediate acquisition times, resulting in this case in a temporal footprint = 6 s.

In Example 2, contrast information is accordingly refreshed every 2 s, while only every 4 s in Example 1. However, Example 1 is the temporally "cleaner" representation, since the temporal footprint is shorter. For TRICKS, TREAT and TWIST the "temporal footprint" is in each case accordingly a multiple of the time duration of an individual dynamic phase and reflects the period of time over which the acquisition of a complete k-space data set extends.

On the other hand, it would not be wise to apply this concept to keyhole-based methods, since the entire peripheral k-space in this instance is acquired only once, which would thus yield periods of differing length for the "temporal footprint", each depending on what point in time the acquisition of the central k-space is observed [28].

Regardless of the technique employed, a high degree of temporal accuracy in the collected dynamic data is desired in clinical applications. Future studies are needed to more accurately examine which technique constitutes the optimal compromise between temporal interpolation, "temporal footprint" and image for a particular clinical problem [105, 106].

For precisely imaging smaller structures, in particular, the signal-time-curve ("point spread function") is ultimately of special importance. Temporal interpolation can result in inferior definition that can manifest itself in, for example, limitations in imaging small arterial supply vessels of arteriovenous malformations [26, 107]. With increasing segmentation, the inferior definition of the peak of the signal-to-time curve becomes more pronounced, which also limits the degree of the possible segmentation steps in the increasingly complex acquisition schemes [73].

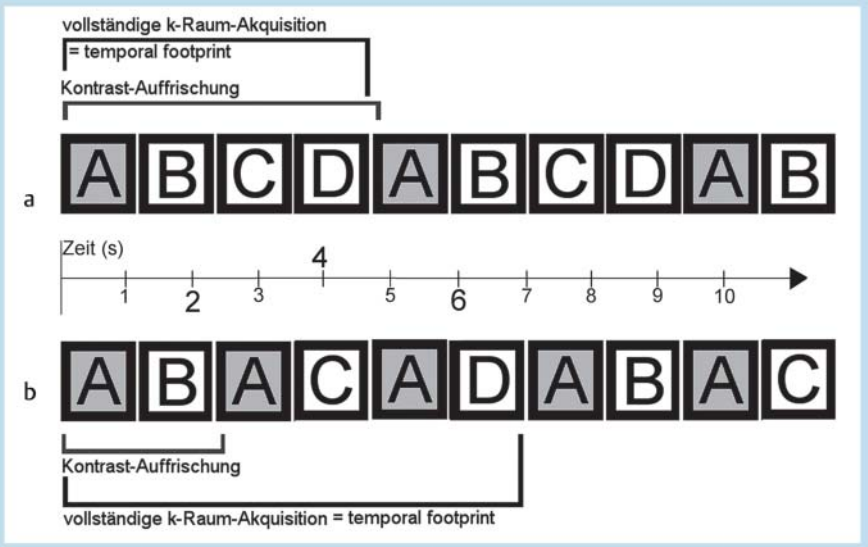

Fig. 3 Image refresh rate (contrast refresh) scheme compared to "temporal footprint" in the case of two different acquisition schemes **a**, **b**.

Clinical perspectives

The technical methods for acquiring 3D-CEMRA image series, some of which are highly complex, are already facilitating detailed observation of numerous pathological changes in flow that were previously the domain of invasive DSA. **Fig. 1b** provides a quantitative overview of which methods have come into use in the past few years. **Fig. 3 – 6** provide several examples of images, while **Table 2** offers an overview of clinical applications to date and shows the multifaceted application possibilities of 4D-MRA. Established routine clinical applications in the meantime include the diagnosis of arteriovenous malformations or fistulae. Unlike conventional static sequences, these applications allow the imaging of premature filling of veins or sinuses by shunt mechanisms. Pathological flow conditions that would otherwise be possible to reconstruct only with invasive methods can likewise be shown in cases of aortic dissections, endoleaks from aortic prostheses or subclavian steal syndrome. Finally, the method sees frequent routine clinical use in generating purely arterial images of the lower leg in cases of asymmetrical arterial filling due to upstream stenoses (in peripheral occlusive arterial disease) or arteriovenous shunts (often in cases of diabetic microangiopathy). In these cases, precise timing for adjusting arterial perfusion and thus a pure arterial 3D-CEMRA is oftentimes not possible.

That cAVM was examined notably using 4D-MRA techniques [23, 26, 61, 69, 72, 103, 150 – 153], can be explained by the fact that on the one hand intracranial vessels are particularly suited given their fundamentally low susceptibility to artefacts in view of the circumscribed examination volume without significant patient movements including breathing. On the other hand, the dynamic information of-

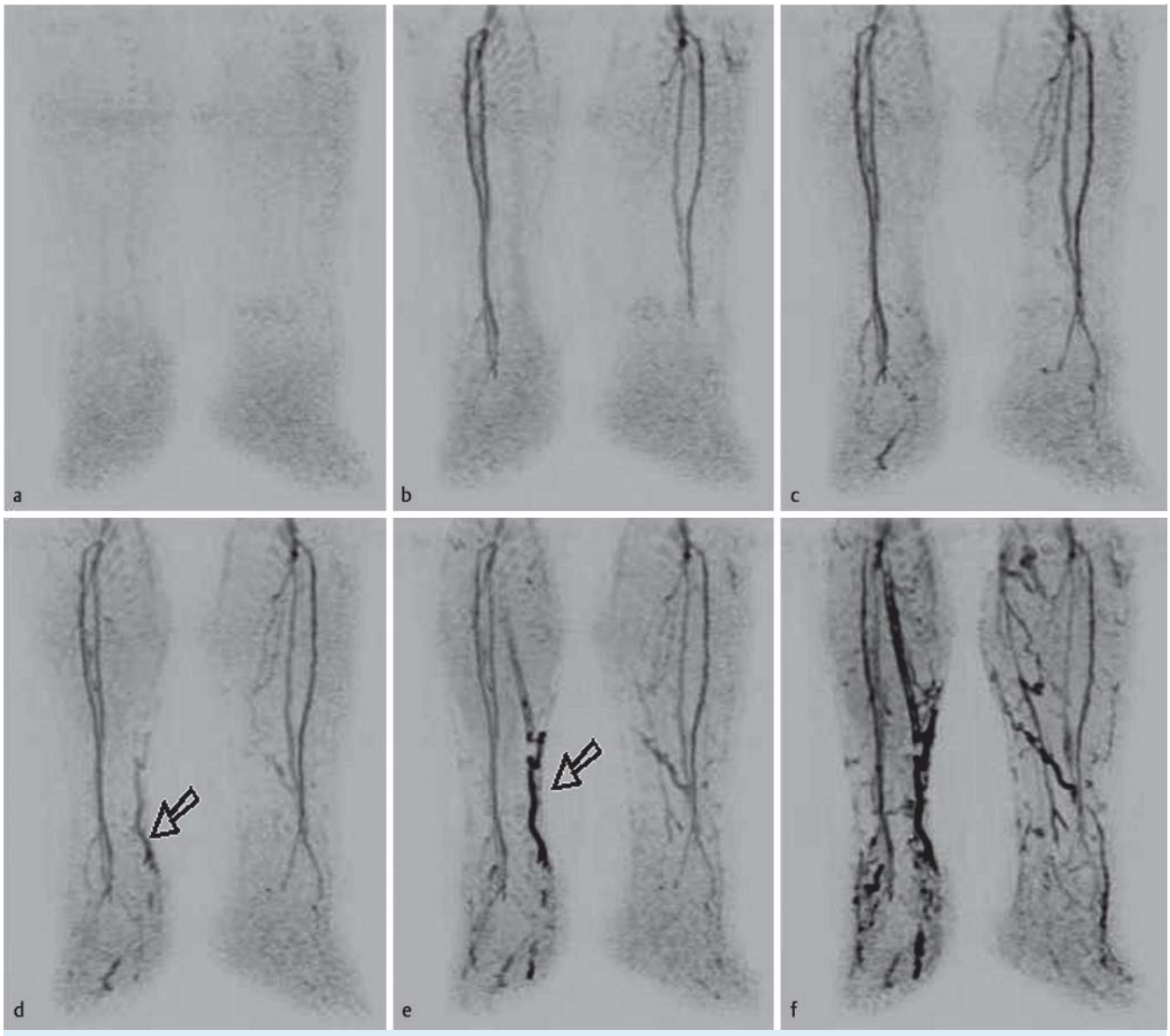

Fig. 4 75-year old patient with stage III peripheral arterial occlusive disease, ambulant < 50 m, complaints primarily on the right side. Total volume maximum intensity projections of high temporal resolution 4D-MRA show the lower legs prior to arrival of contrast agent (**a**), arterial bolus passage (**b**–**d**), and premature venous enhancement in the right lower leg resulting from a shunt between the right peroneal artery (arrows in **d, e**) and the great saphenous vein, as well as venous filling in a later phase **f**.

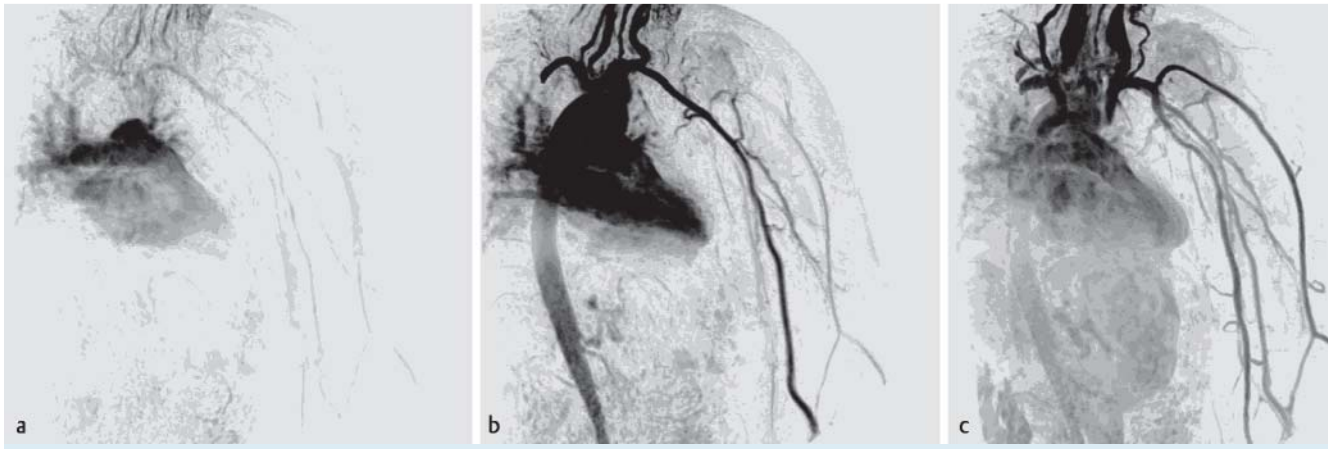

Fig. 5 69-year old female patient with acute swelling of the left arm presenting septic clinical picture, imaging performed to exclude thrombosis. Representative total volume maximum intensity projections per one phase of 4D-MRA prior to arrival of contrast agent bolus **a**, during arterial bolus passage **b** and during venous phase of contrast agent passage **c**.

Table 2 Clinical applications of TR-MRA.

bodily region	clinical problem	references
head	carotids	[95, 114 – 116]
	cerebral arteriovenous fistulae and malformations	[33, 47, 65, 117 – 119]
	cavernous hemangioma	[117, 120]
	sinus thrombosis	[33, 121]
	multiple sclerosis	[122 – 124]
	orbital lesions	[65, 125]
spinal column	spinal arteries	[30, 71, 126]
	arteriovenous fistulae and malformations	[54, 72, 76]
thorax/abdomen	aortic dissection	[17, 127]
	aortic isthmus stenosis	[128]
	pulmonary embolisms	[63]
	pulmonary perfusion	[9, 10, 12, 13, 29]
	pulmonary hypertension	[8, 11]
	arteriovenous malformations	[36, 129]
	endoleaks from vascular prostheses	[82, 130, 131]
	subclavian steal syndrome	[90]
	coronary vessels	[132 – 134]
	renal artery stenoses	[135 – 137]
	pelvic congestion	[32, 57, 98, 138, 139]
arteries of the extremities	asymmetrical contrast perfusion	[56, 99, 140 – 143]
	arteriovenous malformations	[144 – 146]
	diabetic microangiopathy	[31, 147 – 150]

fers especially high potential benefits, and the reference standard of DSA is frequently on hand for comparative purposes.

TR-MRA, however, also opens numerous new diagnostic avenues. For example it is conceivable when using an intravascular contrast agent to first acquire detailed functional information with the aid of TR-MRA (e. g. for diagnosing a pulmonary embolism) and then to image an underlying leg vein thrombosis with the aid of a high-resolution spatial sequence [154, 155]. Primarily intravascularly dwelling contrast agents of this type with reversible protein binding and thereafter considerably delayed pervasion of the interstitium are currently available only in North America.

In the studies on clinical applications of TR-MRA some of which involved high image refresh rates and high spatial resolution, the majority of temporal information was displayed and at the same time the contrast agent dose administered was oftentimes significantly reduced compared to the static, high spatial resolution 3D-CEMRA. In the future, combining echo-sharing techniques with special data reconstruction methods using only a fraction of the actually required data (HYPR, compressed sensing) may possibly allow even significantly higher image refresh rates, thereby facilitating the generation of real-time sequences and detailed examination of flow conditions [156, 157].

Disadvantages compared to DSA resulting from the simultaneous contrast agent perfusion in all vascular segments (a not insignificant advantage of DSA is the possibility of selective contrast agent administration) are compensated partly with a vascular selective excitement using what is known as arterial spin labelling (ASL) [34, 158]. In the future, further insight on flow dynamics may possibly be gained through

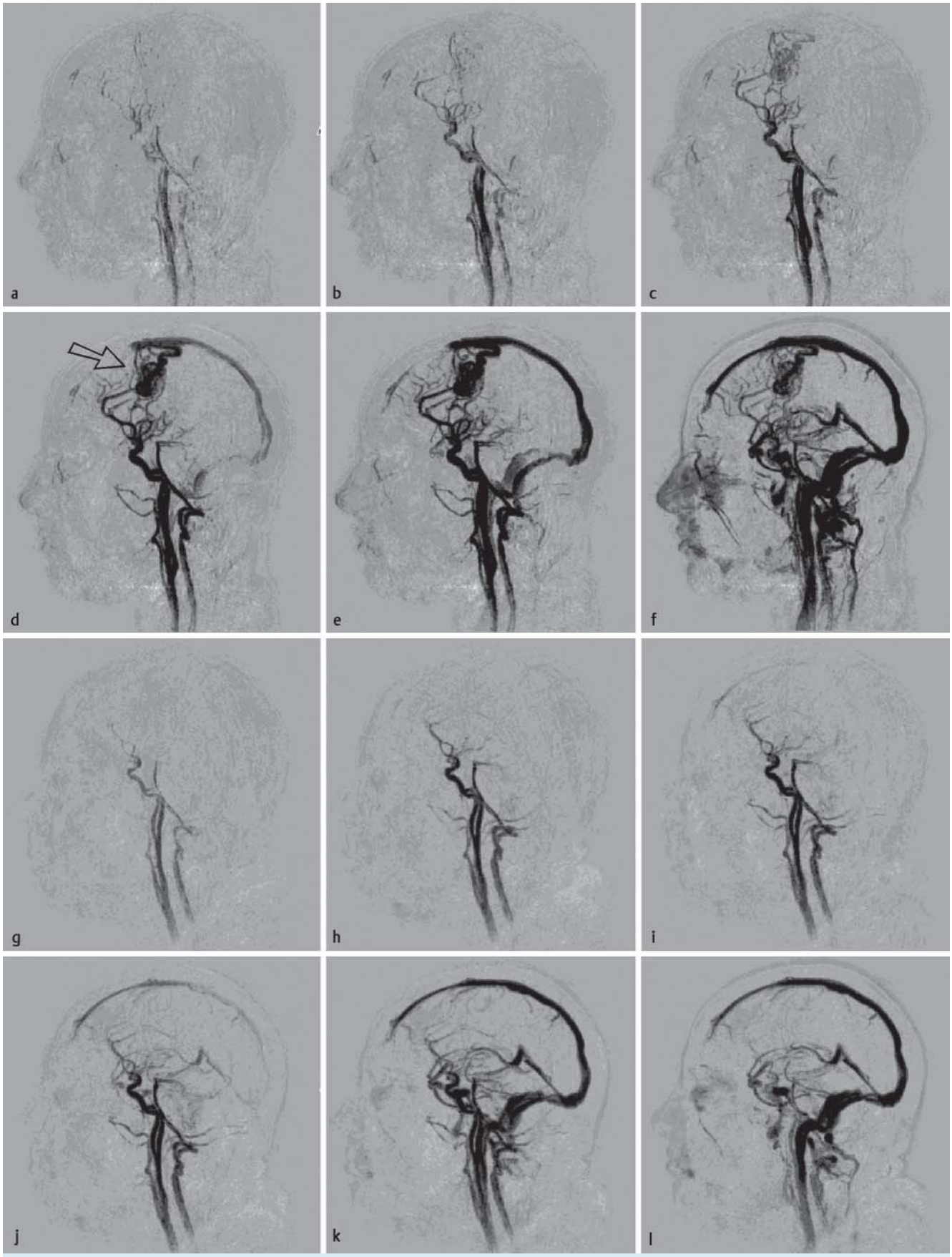

Fig. 6 25-year old male patient before **a – f** and after **g – l** surgical resection of a right frontal cerebral arteriovenous malformation (arrow in **d**) in a non-eloquent area of the brain. Lateral total volume maximum intensity projections of temporally corresponding phases of contrast-enhanced 4D-MRA.

techniques such as high temporal and spatial resolution and at the same time quantitative phase contrast angiography (4D-PC-MRA), which has lately shown considerable promise [159 – 165]. Finally, real-time imaging, for example during catheter interventions with susceptibility markers, is a promising area of application for 4D-MRA. However, this is the subject of predominantly preclinical studies [165, 167].

Summary

TR-MRA was initially used only for facilitating fluoroscopic bolus triggering and gaining exact timing for performing a high spatial resolution static, pure arterial 3D-CEMRA, for instance, of the supra-aortic arteries. With the aid of complex k-space acquisition algorithms, parallel imaging and new echo-sharing techniques while at the same time at higher spatial resolution. This is opening up new areas of application that had mainly eluded non-invasive testing until now. It will be exciting to see what benefits further technological advancements in both coil and scanner technology, such as for example fully digitalized signal transmission and reception, will have for TR-MRA in the future and what importance this innovative technology will have in routine clinical use.

Literatur

1 *Prince MR, Yucel EK, Kaufman JA et al.* Dynamic gadolinium-enhanced three-dimensional abdominal MR arteriography. J Magn Reson Imaging 1993; 3: 877 – 881
2 *Jones RA, Haraldseth O, Muller TB et al.* K-space substitution: a novel dynamic imaging technique. Magn Reson Med 1993; 29: 830 – 834
3 *van Vaals JJ, Brummer ME, Dixon WT et al.* "Keyhole" method for accelerating imaging of contrast agent uptake. J Magn Reson Imaging 1993; 3: 671 – 675
4 *Pruessmann KP, Weiger M, Scheidegger MB et al.* SENSE: sensitivity encoding for fast MRI. Magn Reson Med 1999; 42: 952 – 962
5 *Sodickson DK, Manning WJ.* Simultaneous acquisition of spatial harmonics (SMASH): fast imaging with radiofrequency coil arrays. Magn Reson Med 1997; 38: 591 – 603
6 *Miyazaki M, Lee VS.* Nonenhanced MR angiography. Radiology 2008; 248: 20 – 43
7 *Cornfeld D, Mojibian H.* Clinical uses of time-resolved imaging in the body and peripheral vascular system. Am J Roentgenol 2009; 193: W546 – W557
8 *Jeong HJ, Vakil P, Sheehan JJ et al.* Time-resolved magnetic resonance angiography: Evaluation of intrapulmonary circulation parameters in pulmonary arterial hypertension. J Magn Reson Imaging 2011; 33: 225 – 231
9 *Risse F, Eichinger M, Kauczor HU et al.* Improved visualization of delayed perfusion in lung MRI. Eur J Radiol 2011; 77: 105 – 110
10 *Schoenberg SO, Bock M, Floemer F et al.* High-resolution pulmonary arterio- and venography using multiple-bolus multiphase 3D-Gd-mRA. J Magn Reson Imaging 1999; 10: 339 – 346
11 *Sergiacomi G, Bolacchi F, Cadioli M et al.* Combined pulmonary fibrosis and emphysema: 3D time-resolved MR angiographic evaluation of pulmonary arterial mean transit time and time to peak enhancement. Radiology 2010; 254: 601 – 608
12 *Tomasian A, Krishnam MS, Lohan DG et al.* Adult Tetralogy of Fallot: quantitative assessment of pulmonary perfusion with time-resolved three dimensional magnetic resonance angiography. Invest Radiol 2009; 44: 31 – 37
13 *Tuite DJ, Francois C, Dill K et al.* Diagnosis and characterization of pulmonary sequestration using dynamic time-resolved magnetic resonance angiography. Clin Radiol 2008; 63: 913 – 917
14 *Cai Z, Stolpen A, Sharafuddin MJ et al.* Bolus characteristics based on Magnetic Resonance Angiography. Biomed Eng Online 2006; 5: 53
15 *Kreitner KF, Kunz RP, Weschler C et al.* [Systematic analysis of the geometry of a defined contrast medium bolus – implications for contrast enhanced 3D MR-angiography of thoracic vessels]. Fortschr Röntgenstr 2005; 177: 646 – 654
16 *Wang Y, Johnston DL, Breen JF et al.* Dynamic MR digital subtraction angiography using contrast enhancement, fast data acquisition, and complex subtraction. Magn Reson Med 1996; 36: 551 – 556
17 *Finn JP, Baskaran V, Carr JC et al.* Thorax: low-dose contrast-enhanced three-dimensional MR angiography with subsecond temporal resolution – initial results. Radiology 2002; 224: 896 – 904
18 *Frayne R, Grist TM, Korosec FR et al.* MR angiography with three-dimensional MR digital subtraction angiography. Top Magn Reson Imaging 1996; 8: 366 – 388
19 *Weiger M, Pruessmann KP, Kassner A et al.* Contrast-enhanced 3D MRA using SENSE. J Magn Reson Imaging 2000; 12: 671 – 677
20 *Riederer SJ, Tasciyan T, Farzaneh F et al.* MR fluoroscopy: technical feasibility. Magn Reson Med 1988; 8: 1 – 15
21 *Spielman DM, Pauly JM, Meyer CH.* Magnetic resonance fluoroscopy using spirals with variable sampling densities. Magn Reson Med 1995; 34: 388 – 394
22 *Nael K, Michaely HJ, Lee M et al.* Dynamic pulmonary perfusion and flow quantification with MR imaging, 3.0T vs. 1.5T: initial results. J Magn Reson Imaging 2006; 24: 333 – 339
23 *Ziyeh S, Strecker R, Berlis A et al.* Dynamic 3D MR angiography of intra- and extracranial vascular malformations at 3T: a technical note. Am J Neuroradiol 2005; 26: 630 – 634
24 *Kukuk GM, Hadizadeh DR, Gieseke J et al.* Highly undersampled supraaortic MRA at 3.0 T: initial results with parallel imaging in two directions using a 16-channel neurovascular coil and parallel imaging factors up to 16. Magn Reson Imaging 2010; 28: 1311 – 1318
25 *Willinek WA, Gieseke J, Conrad R et al.* Randomly segmented central k-space ordering in high-spatial-resolution contrast-enhanced MR angiography of the supraaortic arteries: initial experience. Radiology 2002; 225: 583 – 588
26 *Hadizadeh DR, von Falkenhausen M, Gieseke J et al.* Cerebral arteriovenous malformation: Spetzler-Martin classification at subsecond-temporal-resolution four-dimensional MR angiography compared with that at DSA. Radiology 2008; 246: 205 – 213
27 *Willinek WA, Hadizadeh DR, von Falkenhausen M et al.* 4D time-resolved MR angiography with keyhole (4D-TRAK): more than 60 times accelerated MRA using a combination of CENTRA, keyhole, and SENSE at 3.0T. J Magn Reson Imaging 2008; 27: 1455 – 1460
28 *Hadizadeh DR, Gieseke J, Beck G et al.* View-sharing in keyhole imaging: Partially compressed central k-space acquisition in time-resolved MRA at 3.0T. Eur J Radiol 2011; 80: 400 – 406
29 *Beranek-Chiu J, Froehlich JM, Wentz KU et al.* Improved vessel delineation in keyhole time-resolved contrast-enhanced MR angiography using a gadolinium doped flush. J Magn Reson Imaging 2009; 29: 1147 – 1153
30 *Boussel L, Cernicanu A, Geerts L et al.* 4D time-resolved magnetic resonance angiography for noninvasive assessment of pulmonary arteriovenous malformations patency. J Magn Reson Imaging 2010; 32: 1110 – 1116
31 *Frydrychowicz A, Bley TA, Zadeh ZA et al.* Image analysis in time-resolved large field of view 3D MR-angiography at 3T. J Magn Reson Imaging 2008; 28: 1116 – 1124
32 *Horie T, Honda M, Okumura Y et al.* Basic examination of CEMRA with 4D time-resolved angiography using keyhole (4D-TRAK) in 3T pelvic region. Nippon Hoshasen Gijutsu Gakkai Zasshi 2008; 64: 1532 – 1539
33 *Itou D, Nagasaka T, Yanagawa I et al.* Use of the keyhole technique for 3.0T MRI dynamic imaging. Nippon Hoshasen Gijutsu Gakkai Zasshi 2008; 64: 1562 – 1567
34 *Kukuk GM, Hadizadeh DR, Bostrom A et al.* Cerebral arteriovenous malformations at 3.0 T: intraindividual comparative study of 4D-MRA in combination with selective arterial spin labeling and digital subtraction angiography. Invest Radiol 2010; 45: 126 – 132
35 *Langer S, Kramer N, Mommertz G et al.* Unmasking pedal arteries in patients with critical ischemia using time-resolved contrast-enhanced 3D MRA. J Vasc Surg 2009; 49: 1196 – 1202
36 *Nishimura S, Hirai T, Sasao A et al.* Evaluation of dural arteriovenous fistulas with 4D contrast-enhanced MR angiography at 3T. Am J Neuroradiol 2010; 31: 80 – 85
37 *Parmar H, Ivancevic MK, Dudek N et al.* Dynamic MRA with four-dimensional time-resolved angiography using keyhole at 3 tesla in head and neck vascular lesions. J Neuroophthalmol 2009; 29: 119 – 127

38 *Raoult H, Ferre JC, Morandi X et al.* Quality-evaluation scheme for cerebral time-resolved 3D contrast-enhanced MR angiography techniques. Am J Neuroradiol 2010; 31: 1480 – 1487
39 *Reinacher PC, Stracke P, Reinges MH et al.* Contrast-enhanced time-resolved 3-D MRA: applications in neurosurgery and interventional neuroradiology. Neuroradiology 2007; 49: S3 – S13
40 *Ruhl KM, Katoh M, Langer S et al.* Time-resolved 3D MR angiography of the foot at 3 T in patients with peripheral arterial disease. Am J Roentgenol 2008; 190: W360 – W364
41 *Hadizadeh DR, Kukuk GM, Steck DT et al.* Noninvasive evaluation of cerebral arteriovenous malformations by 4D-MRA for preoperative planning and postoperative follow-up in 56 patients: comparison with DSA and intraoperative findings. Am J Neuroradiol 2012; 33: 1095 – 1101
42 *Korosec FR, Frayne R, Grist TM et al.* Time-resolved contrast-enhanced 3D MR angiography. Magn Reson Med 1996; 36: 345 – 351
43 *Du YP, Parker DL, Davis WL et al.* Reduction of partial-volume artifacts with zero-filled interpolation in three-dimensional MR angiography. J Magn Reson Imaging 1994; 4: 733 – 741
44 *Vigen KK, Peters DC, Grist TM et al.* Undersampled projection-reconstruction imaging for time-resolved contrast-enhanced imaging. Magn Reson Med 2000; 43: 170 – 176
45 *Huang Y, Wright GA.* Time-resolved MR angiography with limited projections. Magn Reson Med 2007; 58: 316 – 325
46 *Wu Y, Johnson K, Kecskemeti SR et al.* Time resolved contrast enhanced intracranial MRA using a single dose delivered as sequential injections and highly constrained projection reconstruction (HYPR CE). Magn Reson Med 2011; 65: 956 – 963
47 *Du J, Carroll TJ, Wagner HJ et al.* Time-resolved, undersampled projection reconstruction imaging for high-resolution CE-MRA of the distal runoff vessels. Magn Reson Med 2002; 48: 516 – 522
48 *Ali S, Cashen TA, Carroll TJ et al.* Time-resolved spinal MR angiography: initial clinical experience in the evaluation of spinal arteriovenous shunts. Am J Neuroradiol 2007; 28: 1806 – 1810
49 *Andreisek G, Pfammatter T, Goepfert K et al.* Peripheral arteries in diabetic patients: standard bolus-chase and time-resolved MR angiography. Radiology 2007; 242: 610 – 620
50 *Archambault E, Gouny P, Hebert T et al.* MR angiography of peripheral arterial disease of the distal legs: is time resolved MRA (TRICKS) necessary? J Radiol 2008; 89: 863 – 871
51 *Dick EA, Burnett C, Anstee A et al.* Time-resolved imaging of contrast kinetics three-dimensional (3D) magnetic resonance venography in patients with pelvic congestion syndrome. Br J Radiol 2010; 83: 882 – 887
52 *Du J, Korosec FR, Thornton FJ et al.* High-resolution multistation peripheral MR angiography using undersampled projection reconstruction imaging. Magn Reson Med 2004; 52: 204 – 208
53 *Du J, Thornton FJ, Mistretta CA et al.* Dynamic MR venography: an intrinsic benefit of time-resolved MR angiography. J Magn Reson Imaging 2006; 24: 922 – 927
54 *Du J, Fain SB, Korosec FR et al.* Time-resolved contrast-enhanced carotid imaging using undersampled projection reconstruction acquisition. J Magn Reson Imaging 2007; 25: 1093 – 1099
55 *Du J, Bydder M.* High-resolution time-resolved contrast-enhanced MR abdominal and pulmonary angiography using a spiral-TRICKS sequence. Magn Reson Med 2007; 58: 631 – 635
56 *Ersoy H, Zhang H, Prince MR.* Peripheral MR angiography. J Cardiovasc Magn Reson 2006; 8: 517 – 528
57 *Ersoy H, Goldhaber SZ, Cai T et al.* Time-resolved MR angiography: a primary screening examination of patients with suspected pulmonary embolism and contraindications to administration of iodinated contrast material. Am J Roentgenol 2007; 188: 1246 – 1254
58 *Fink C, Puderbach M, Ley S et al.* Intraindividual comparison of 1.0 M gadobutrol and 0.5 M gadopentetate dimeglumine for time-resolved contrast-enhanced three-dimensional magnetic resonance angiography of the upper torso. J Magn Reson Imaging 2005; 22: 286 – 290
59 *Kahana A, Lucarelli MJ, Grayev AM et al.* Noninvasive dynamic magnetic resonance angiography with Time-Resolved Imaging of Contrast KineticS (TRICKS) in the evaluation of orbital vascular lesions. Arch Ophthalmol 2007; 125: 1635 – 1642
60 *Mell M, Tefera G, Thornton F et al.* Clinical utility of time-resolved imaging of contrast kinetics (TRICKS) magnetic resonance angiography for infrageniculate arterial occlusive disease. J Vasc Surg 2007; 45: 543 – 548
61 *Petkova M, Gauvrit JY, Trystram D et al.* Three-dimensional dynamic time-resolved contrast-enhanced MRA using parallel imaging and a variable rate k-space sampling strategy in intracranial arteriovenous malformations. J Magn Reson Imaging 2009; 29: 7 – 12
62 *Thornton FJ, Du J, Suleiman SA et al.* High-resolution, time-resolved MRA provides superior definition of lower-extremity arterial segments compared to 2D time-of-flight imaging. J Magn Reson Imaging 2006; 24: 362 – 370
63 *Vattoth S, Cherian J, Pandey T.* Magnetic resonance angiographic demonstration of carotid-cavernous fistula using elliptical centric time resolved imaging of contrast kinetics (EC-TRICKS). Magn Reson Imaging 2007; 25: 1227 – 1231
64 *Wang CC, Liang HL, Hsiao CC et al.* Single-dose time-resolved contrast enhanced hybrid MR angiography in diagnosis of peripheral arterial disease: compared with digital subtraction angiography. J Magn Reson Imaging 2010; 32: 935 – 942
65 *Bley TA, Duffek CC, Francois CJ et al.* Presurgical localization of the artery of Adamkiewicz with time-resolved 3.0-T MR angiography. Radiology 2010; 255: 873 – 881
66 *Boeckh-Behrens T, Bitterling H, Schichor C et al.* Improved localization of spinal AV fistulas using contrast-enhanced MR angiography at 3 T. Fortschr Röntgenstr 2010; 182: 53 – 57
67 *Farb RI, Agid R, Willinsky RA et al.* Cranial dural arteriovenous fistula: diagnosis and classification with time-resolved MR angiography at 3T. Am J Neuroradiol 2009; 30: 1546 – 1551
68 *Ganguli S, Pedrosa I, Smith MP et al.* Low dose pedal magnetic resonance angiography at 3 tesla with time-resolved imaging of contrast kinetics: a feasibility study. Invest Radiol 2008; 43: 650 – 655
69 *Kunishima K, Mori H, Itoh D et al.* Assessment of arteriovenous malformations with 3-Tesla time-resolved, contrast-enhanced, three-dimensional magnetic resonance angiography. J Neurosurg 2009; 110: 492 – 499
70 *Riccioli LA, Marliani AF, Ghedin P et al.* CE-MR Angiography at 3.0 T Magnetic Field in the Study of Spinal Dural Arteriovenous Fistula. Preliminary Results. Interv Neuroradiol 2007; 13: 13 – 18
71 *Sakamoto S, Shibukawa M, Kiura Y et al.* Evaluation of dural arteriovenous fistulas of cavernous sinus before and after endovascular treatment using time-resolved MR angiography. Neurosurg Rev 2010; 33: 217 – 222
72 *Zou Z, Ma L, Cheng L et al.* Time-resolved contrast-enhanced MR angiography of intracranial lesions. J Magn Reson Imaging 2008; 27: 692 – 699
73 *Fink C, Ley S, Kroeker R et al.* Time-resolved contrast-enhanced three-dimensional magnetic resonance angiography of the chest: combination of parallel imaging with view sharing (TREAT). Invest Radiol 2005; 40: 40 – 48
74 *Griswold MA, Jakob PM, Heidemann RM et al.* Generalized autocalibrating partially parallel acquisitions (GRAPPA). Magn Reson Med 2002; 47: 1202 – 1210
75 *Brauck K, Maderwald S, Vogt FM et al.* Time-resolved contrast-enhanced magnetic resonance angiography of the hand with parallel imaging and view sharing: initial experience. Eur Radiol 2007; 17: 183 – 192
76 *Cohen EI, Weinreb DB, Siegelbaum RH et al.* Time-resolved MR angiography for the classification of endoleaks after endovascular aneurysm repair. J Magn Reson Imaging 2008; 27: 500 – 503
77 *Fink C, Puderbach M, Ley S et al.* Time-resolved echo-shared parallel MRA of the lung: observer preference study of image quality in comparison with non-echo-shared sequences. Eur Radiol 2005; 15: 2070 – 2074
78 *Gauvrit JY, Law M, Xu J et al.* Time-resolved MR angiography: optimal parallel imaging method. Am J Neuroradiol 2007; 28: 835 – 838
79 *Kim CY, Mirza RA, Bryant JA et al.* Central veins of the chest: evaluation with time-resolved MR angiography. Radiology 2008; 247: 558 – 566
80 *Kramer H, Michaely HJ, Requardt M et al.* Effects of injection rate and dose on image quality in time-resolved magnetic resonance angiography (MRA) by using 1.0M contrast agents. Eur Radiol 2007; 17: 1394 – 1402
81 *Krishnam MS, Tomasian A, Lohan DG et al.* Low-dose, time-resolved, contrast-enhanced 3D MR angiography in cardiac and vascular diseases: correlation to high spatial resolution 3D contrast-enhanced MRA. Clin Radiol 2008; 63: 744 – 755
82 *Lee MW, Lee JM, Lee JY et al.* Preoperative evaluation of hepatic arterial and portal venous anatomy using the time resolved echo-shared MR angiographic technique in living liver donors. Eur Radiol 2007; 17: 1074 – 1080
83 *Ley S, Fink C, Zaporozhan J et al.* Value of high spatial and high temporal resolution magnetic resonance angiography for differentiation between idiopathic and thromboembolic pulmonary hypertension: initial results. Eur Radiol 2005; 15: 2256 – 2263

84 *Virmani R*, *Carroll TJ*, *Hung J et al.* Diagnosis of subclavian steal syndrome using dynamic time-resolved magnetic resonance angiography: a technical note. Magn Reson Imaging 2008; 26: 287 – 292
85 *Cashen TA*, *Carr JC*, *Shin W et al.* Intracranial time-resolved contrast-enhanced MR angiography at 3T. Am J Neuroradiol 2006; 27: 822 – 829
86 *Frydrychowicz A*, *Bley TA*, *Winterer JT et al.* Accelerated time-resolved 3D contrast-enhanced MR angiography at 3T: clinical experience in 31 patients. MAGMA 2006; 19: 187 – 195
87 *Nael K*, *Michaely HJ*, *Villablanca P et al.* Time-resolved contrast enhanced magnetic resonance angiography of the head and neck at 3.0 tesla: initial results. Invest Radiol 2006; 41: 116 – 124
88 *Saleh RS*, *Lohan DG*, *Villablanca JP et al.* Assessment of craniospinal arteriovenous malformations at 3T with highly temporally and highly spatially resolved contrast-enhanced MR angiography. Am J Neuroradiol 2008; 29: 1024 – 1031
89 *Lim RP*, *Shapiro M*, *Wang EY et al.* 3D time-resolved MR angiography (MRA) of the carotid arteries with time-resolved imaging with stochastic trajectories: comparison with 3D contrast-enhanced Bolus-Chase MRA and 3D time-of-flight MRA. Am J Neuroradiol 2008; 29: 1847 – 1854
90 *Vogt FM*, *Eggebrecht H*, *Laub G et al.* High spatial and temporal resolution MRA (TWIST) in acute aortic dissection. Proc Intl Soc Mag Reson Med 2007; 15: 92
91 *Song T*, *Laine AF*, *Chen Q et al.* Optimal k-space sampling for dynamic contrast-enhanced MRI with an application to MR renography. Magn Reson Med 2009; 61: 1242 – 1248
92 *Kim CY*, *Miller MJ Jr*, *Merkle EM*. Time-resolved MR angiography as a useful sequence for assessment of ovarian vein reflux. Am J Roentgenol 2009; 193: W458 – W463
93 *Lim RP*, *Jacob JS*, *Hecht EM et al.* Time-resolved lower extremity MRA with temporal interpolation and stochastic spiral trajectories: preliminary clinical experience. J Magn Reson Imaging 2010; 31: 663 – 672
94 *Nael K*, *Krishnam M*, *Ruehm SG et al.* Time-resolved MR angiography in the evaluation of central thoracic venous occlusive disease. Am J Roentgenol 2009; 192: 1731 – 1738
95 *Sandhu GS*, *Rezaee RP*, *Wright K et al.* Time-resolved and bolus-chase MR angiography of the leg: branching pattern analysis and identification of septocutaneous perforators. Am J Roentgenol 2010; 195: 858 – 864
96 *Seng K*, *Maderwald S*, *de Greiff A et al.* Dynamic contrast-enhanced magnetic resonance angiography of the thoracic vessels: an intraindividual comparison of different k-space acquisition strategies. Invest Radiol 2010; 45: 708 – 714
97 *Attenberger UI*, *Haneder S*, *Morelli JN et al.* Peripheral arterial occlusive disease: evaluation of a high spatial and temporal resolution 3-T MR protocol with a low total dose of gadolinium versus conventional angiography. Radiology 2010; 257: 879 – 887
98 *Giesel FL*, *Runge V*, *Kirchin M et al.* Three-dimensional multiphase time-resolved low-dose contrast-enhanced magnetic resonance angiography using TWIST on a 32-channel coil at 3 T: a quantitative and qualitative comparison of a conventional gadolinium chelate with a high-relaxivity agent. J Comput Assist Tomogr 2010; 34: 678 – 683
99 *Koktzoglou I*, *Sheehan JJ*, *Dunkle EE et al.* Highly accelerated contrast-enhanced MR angiography: improved reconstruction accuracy and reduced noise amplification with complex subtraction. Magn Reson Med 2010; 64: 1843 – 1848
100 *Kramer U*, *Fenchel M*, *Laub G et al.* Low-dose, time-resolved, contrast-enhanced 3D MR angiography in the assessment of the abdominal aorta and its major branches at 3 Tesla. Acad Radiol 2010; 17: 564 – 576
101 *Lee YJ*, *Laub G*, *Jung SL et al.* Low-dose 3D time-resolved magnetic resonance angiography (MRA) of the supraaortic arteries: Correlation with high spatial resolution 3D contrast-enhanced MRA. J Magn Reson Imaging 2011; 33: 71 – 76
102 *Li D*, *Lin J*, *Yan F et al.* Unenhanced calf MR angiography at 3.0 T using electrocardiography-gated partial-fourier fast spin echo imaging with variable flip angle. Eur Radiol 2010; 21: 1311 – 1322
103 *Oleaga L*, *Dalal SS*, *Weigele JB et al.* The role of time-resolved 3D contrast-enhanced MR angiography in the assessment and grading of cerebral arteriovenous malformations. Eur J Radiol 2010; 74: e117 – e121
104 *Voth M*, *Haneder S*, *Huck K et al.* Peripheral magnetic resonance angiography with continuous table movement in combination with high spatial and temporal resolution time-resolved MRA With a total single dose (0.1 mmol/kg) of gadobutrol at 3.0 T. Invest Radiol 2009; 44: 627 – 633
105 *Jeong HJ*, *Eddleman CS*, *Shah S et al.* Accelerating time-resolved MRA with multiecho acquisition. Magn Reson Med 2010; 63: 1520 – 1528
106 *Riederer SJ*, *Haider CR*, *Borisch EA*. Time-of-arrival mapping at three-dimensional time-resolved contrast-enhanced MR angiography. Radiology 2009; 253: 532 – 542
107 *Reinacher P*, *Reinges MH*, *Simon VA et al.* Dynamic 3-D contrast-enhanced angiography of cerebral tumours and vascular malformations. Eur Radiol 2007; 17: F52 – F62
108 *Fellner C*, *Lang W*, *Janka R et al.* Magnetic resonance angiography of the carotid arteries using three different techniques: accuracy compared with intraarterial x-ray angiography and endarterectomy specimens. J Magn Reson Imaging 2005; 21: 424 – 431
109 *Lenhart M*, *Finkenzeller T*, *Paetzel C et al.* Contrast-enhanced MR angiography in the routine work-up of the lower extremity arteries. Fortschr Röntgenstr 2002; 174: 1289 – 1295
110 *Sasaki M*, *Oikawa H*, *Yoshioka K et al.* Combining time-resolved and single-phase 3D techniques in contrast-enhanced carotid MR angiography. Magn Reson Med Sci 2002; 1: 1 – 6
111 *Spuentrup E*, *Wiethoff AJ*, *Parsons EC et al.* High spatial resolution magnetic resonance imaging of experimental cerebral venous thrombosis with a blood pool contrast agent. Eur J Radiol 2010; 74: 445 – 452
112 *Shim YW*, *Chung TS*, *Kang WS et al.* Hemodynamical assessment of cavernous hemangioma in cavernous sinus using MR-DSA and conventional DSA. Yonsei Med J 2003; 44: 908 – 914
113 *Illies T*, *Forkert ND*, *Saering D et al.* Persistent hemodynamic changes in ruptured brain arteriovenous malformations. Stroke 2012; 43: 2910 – 2915
114 *Bink A*, *Berkefeld J*, *Wagner M et al.* Detection and grading of dAVF: prospects and limitations of 3T MRI. Eur Radiol 2012; 22: 429 – 438
115 *Kim JS*, *Chandler A*, *Borzykowski R et al.* Maximizing time-resolved MRA for differentiation of hemangiomas, vascular malformations and vascularized tumors. Pediatr Radiol 2012; 42: 775 – 784
116 *Yigit H*, *Turan A*, *Ergun E et al.* Time-resolved MR angiography of the intracranial venous system: an alternative MR venography technique. Eur Radiol 2012; 22: 980 – 989
117 *Utriainen D*, *Feng W*, *Elias S et al.* Using magnetic resonance imaging as a means to study chronic cerebral spinal venous insufficiency in multiple sclerosis patients. Tech Vasc Interv Radiol 2012; 15: 101 – 112
118 *Feng W*, *Utriainen D*, *Trifan G et al.* Quantitative flow measurements in the internal jugular veins of multiple sclerosis patients using magnetic resonance imaging. Rev Recent Clin Trials 2012; 7: 117 – 126
119 *Haacke EM*, *Feng W*, *Utriainen D et al.* Patients with multiple sclerosis with structural venous abnormalities on MR imaging exhibit an abnormal flow distribution of the internal jugular veins. J Vasc Interv Radiol 2012; 23: 60 – 68
120 *Ramey NA*, *Lucarelli MJ*, *Gentry LR et al.* Clinical usefulness of orbital and facial Time-Resolved Imaging of Contrast KineticS (TRICKS) magnetic resonance angiography. Ophthal Plast Reconstr Surg 2012; 28: 361 – 368
121 *Jaspers K*, *Nijenhuis RJ*, *Backes WH*. Differentiation of spinal cord arteries and veins by time-resolved MR angiography. J Magn Reson Imaging 2007; 26: 31 – 40
122 *Iwakura T*, *Takehara Y*, *Yamashita S et al.* A case of paraspinal arteriovenous fistula in the lumbar spinal body assessed with time resolved three-dimensional phase contrast MRI. J Magn Reson Imaging 2012; 36: 1231 – 1233
123 *Schoenberg SO*, *Wunsch C*, *Knopp MV et al.* Abdominal aortic aneurysm. Detection of multilevel vascular pathology by time-resolved multiphase 3D gadolinium MR angiography: initial report. Invest Radiol 1999; 34: 648 – 659
124 *Salanitri GC*. Intercostal artery aneurysms complicating thoracic aortic coarctation: diagnosis with magnetic resonance angiography. Australas Radiol 2007; 51: 78 – 82
125 *Goo HW*, *Yang DH*, *Park IS et al.* Time-resolved three-dimensional contrast-enhanced magnetic resonance angiography in patients who have undergone a Fontan operation or bidirectional cavopulmonary connection: initial experience. J Magn Reson Imaging 2007; 25: 727 – 736
126 *Goyen M*, *Ruehm SG*, *Jagenburg A et al.* Pulmonary arteriovenous malformation: Characterization with time-resolved ultrafast 3D MR angiography. J Magn Reson Imaging 2001; 13: 458 – 460
127 *van der Laan MJ*, *Bakker CJ*, *Blankensteijn JD et al.* Dynamic CE-MRA for endoleak classification after endovascular aneurysm repair. Eur J Vasc Endovasc Surg 2006; 31: 130 – 135

128 *Lookstein RA, Goldman J, Pukin L et al.* Time-resolved magnetic resonance angiography as a noninvasive method to characterize endoleaks: initial results compared with conventional angiography. J Vasc Surg 2004; 39: 27 – 33
129 *Ge L, Bi X, Lai P et al.* Time-resolved contrast-enhanced coronary magnetic resonance angiography with highly constrained projection reconstruction. Magn Reson Imaging 2010; 28: 195 – 199
130 *Lai P, Huang F, Li Y et al.* Contrast-kinetics-resolved whole-heart coronary MRA using 3DPR. Magn Reson Med 2010; 63: 970 – 978
131 *Suever JD, Watson PJ, Eisner RL et al.* Time-resolved analysis of coronary vein motion and cross-sectional area. J Magn Reson Imaging 2011; 34: 811 – 815
132 *Vakil P, Carr JC, Carroll TJ.* Combined renal MRA and perfusion with a single dose of contrast. Magn Reson Imaging 2012; 30: 878 – 885
133 *Morelli JN, Ai F, Runge VM et al.* Time-resolved MR angiography of renal artery stenosis in a swine model at 3 Tesla using gadobutrol with digital subtraction angiography correlation. J Magn Reson Imaging 2012; 36: 704 – 713
134 *Morelli JN, Runge VM, Ai F et al.* Magnetic resonance evaluation of renal artery stenosis in a swine model: performance of low-dose gadobutrol versus gadoterate meglumine in comparison with digital subtraction intra-arterial catheter angiography. Invest Radiol 2012; 47: 376 – 382
135 *Ganeshan A, Upponi S, Hon LQ et al.* Chronic pelvic pain due to pelvic congestion syndrome: the role of diagnostic and interventional radiology. Cardiovasc Intervent Radiol 2007; 30: 1105 – 1111
136 *Pandey T, Shaikh R, Viswamitra S et al.* Use of time resolved magnetic resonance imaging in the diagnosis of pelvic congestion syndrome. J Magn Reson Imaging 2010; 32: 700 – 704
137 *Yang DM, Kim HC, Nam DH et al.* Time-resolved MR angiography for detecting and grading ovarian venous reflux: comparison with conventional venography. Br J Radiol 2012; 85: e117 – e122
138 *Tongdee R, Narra VR, McNeal G et al.* Hybrid peripheral 3D contrast-enhanced MR angiography of calf and foot vasculature. Am J Roentgenol 2006; 186: 1746 – 1753
139 *Wang Y, Chen CZ, Chabra SG et al.* Bolus arterial-venous transit in the lower extremity and venous contamination in bolus chase three-dimensional magnetic resonance angiography. Invest Radiol 2002; 37: 458 – 463
140 *Floery D, Fellner FA, Fellner C et al.* Time-Resolved Contrast-Enhanced MR Angiography of the Lower Limbs: Solving the Problem of Venous Overlap. Fortschr Röntgenstr 2010; DOI: 10.1055/s-0029-1245722
141 *Floery D, Fellner FA, Fellner C et al.* Time-resolved contrast-enhanced MR angiography of the lower limbs: solving the problem of venous overlap. Fortschr Röntgenstr 2011; 183: 136 – 143
142 *Kramer U, Ernemann U, Fenchel M et al.* Pretreatment evaluation of peripheral vascular malformations using low-dose contrast-enhanced time-resolved 3D MR angiography: initial results in 22 patients. Am J Roentgenol 2011; 196: 702 – 711
143 *Mostardi PM, Young PM, McKusick MA et al.* High temporal and spatial resolution imaging of peripheral vascular malformations. J Magn Reson Imaging 2012; 36: 933 – 942
144 *Kramer U, Ernemann U, Mangold S et al.* Diagnostic value of high spatial and temporal resolution time-resolved MR angiography in the workup of peripheral high-flow vascular malformations at 1.5 Tesla. Int J Cardiovasc Imaging 2012; 28: 823 – 834
145 *Mende KA, Froehlich JM, von Weymarn C et al.* Time-resolved, high-resolution contrast-enhanced MR angiography of dialysis shunts using the CENTRA keyhole technique with parallel imaging. J Magn Reson Imaging 2007; 25: 832 – 840
146 *Nicolas M, Laurent V, Tissier S et al.* Dynamic evaluation of lower limb arteries using the ECTRICKS MRI technique. J Radiol 2005; 86: 49 – 59
147 *Planken RN, Tordoir JH, Dammers R et al.* Stenosis detection in forearm hemodialysis arteriovenous fistulae by multiphase contrast-enhanced magnetic resonance angiography: preliminary experience. J Magn Reson Imaging 2003; 17: 54 – 64
148 *Zhang HL, Kent KC, Bush HL et al.* Soft tissue enhancement on time-resolved peripheral magnetic resonance angiography. J Magn Reson Imaging 2004; 19: 590 – 597
149 *Andrade-Souza YM, Zadeh G, Ramani M et al.* Testing the radiosurgery-based arteriovenous malformation score and the modified spetzler-martin grading system to predict radiosurgical outcome. J Neurosurg 2005; 103: 642 – 648
150 *Saleh RS, Singhal A, Lohan D et al.* Assessment of cerebral arteriovenous malformations with high temporal and spatial resolution contrast-enhanced magnetic resonance angiography: a review from protocol to clinical application. Top Magn Reson Imaging 2008; 19: 251 – 257
151 *Klisch J, Strecker R, Hennig J et al.* Time-resolved projection MRA: clinical application in intracranial vascular malformations. Neuroradiology 2000; 42: 104 – 107
152 *Shim YW, Chung TS, Kang WS et al.* Non-invasive follow-up evaluation of post-embolized AVM with time-resolved MRA: a case report. Korean J Radiol 2002; 3: 271 – 275
153 *Taschner CA, Gieseke J, Le T et al.* Intracranial arteriovenous malformation: time-resolved contrast-enhanced MR angiography with combination of parallel imaging, keyhole acquisition, and k-space sampling techniques at 1.5 T. Radiology 2008; 246: 871 – 879
154 *Fink C, Bock M, Kiessling F et al.* Time-resolved contrast-enhanced three-dimensional pulmonary MR-angiography: 1.0 M gadobutrol vs. 0.5 M gadopentetate dimeglumine. J Magn Reson Imaging 2004; 19: 202 – 208
155 *Hoffmann U, Schima W, Herold C.* Pulmonary magnetic resonance angiography. Eur Radiol 1999; 9: 1745 – 1754
156 *Grist TM, Mistretta CA, Strother CM et al.* Time-resolved angiography: Past, present, and future. J Magn Reson Imaging 2012; 36: 1273 – 1286
157 *Lustig M, Donoho D, Pauly JM.* Sparse MRI: The application of compressed sensing for rapid MR imaging. Magn Reson Med 2007; 58: 1182 – 1195
158 *Eddleman CS, Jeong HJ, Hurley MC et al.* 4D radial acquisition contrast-enhanced MR angiography and intracranial arteriovenous malformations: quickly approaching digital subtraction angiography. Stroke 2009; 40: 2749 – 2753
159 *Yamashita S, Isoda H, Hirano M et al.* Visualization of hemodynamics in intracranial arteries using time-resolved three-dimensional phase-contrast MRI. J Magn Reson Imaging 2007; 25: 473 – 478
160 *Schubert T, Santini F, Stalder AF et al.* Dampening of Blood-Flow Pulsatility along the Carotid Siphon: Does Form Follow Function? Am J Neuroradiol 2011; 32: 1107 – 1112
161 *Bock J, Frydrychowicz A, Stalder AF et al.* 4D phase contrast MRI at 3 T: effect of standard and blood-pool contrast agents on SNR, PC-MRA, and blood flow visualization. Magn Reson Med 2010; 63: 330 – 338
162 *Hope TA, Herfkens RJ.* Imaging of the thoracic aorta with time-resolved three-dimensional phase-contrast MRI: a review. Semin Thorac Cardiovasc Surg 2008; 20: 358 – 364
163 *Liu X, Weale P, Reiter G et al.* Breathhold time-resolved three-directional MR velocity mapping of aortic flow in patients after aortic valve-sparing surgery. J Magn Reson Imaging 2009; 29: 569 – 575
164 *Markl M, Harloff A, Bley TA et al.* Time-resolved 3D MR velocity mapping at 3T: improved navigator-gated assessment of vascular anatomy and blood flow. J Magn Reson Imaging 2007; 25: 824 – 831
165 *Frydrychowicz A, Francois CJ, Turski PA.* Four-dimensional phase contrast magnetic resonance angiography: Potential clinical applications. Eur J Radiol 2011; 80: 24 – 35
166 *Saybasili H, Faranesh AZ, Saikus CE et al.* Interventional MRI using multiple 3D angiography roadmaps with real-time imaging. J Magn Reson Imaging 2010; 31: 1015 – 1019
167 *Seppenwoolde JH, Bartels LW, van der Weide R.* Fully MR-guided hepatic artery catheterization for selective drug delivery: a feasibility study in pigs. J Magn Reson Imaging 2006; 23: 123 – 129